Iraqi Journal of Science, 2025, Vol. 66, No. 11, pp: 4768- 4781
DOI: 10.24996/ijs.2025.66.11.7

ISSN: 0067-2904

DFT computations and Experimental research for Corrosion Inhibition of Carbon Steel Surface in Salinized Media Using a Novel Derivative of 2-aryl imidazo [2,1-b] Benzothiazole

Rehab Majed Kubba, Nada Mohammed Al-Joborry*, Naeemah J. Al-lami
Department of Chemistry, College of Science, University of Baghdad, Baghdad, Iraq.

Received: 12/3/2024 Accepted: 10/11/2024 Published: 30/11/2025

Abstract

The study aims to investigate the inhibition efficiency of new 2-aryl imidazo[2,1-b] benzothiazole derivative namely 2- (4-bromophenyl-4-yl)-5 -yl-methylene-3- (p-tolyl)-2- phenyl- (3,5-dihydroimidazoline-4-one) imidazo [2,1-b]benz[d]thiazol (BPMDIB). Quantum chemical calculations were employed to investigate the impact of BPMDIB on carbon steel corrosion. The results showed that increasing the inhibitor concentration resulted in a substantial decrease in the corrosion rate of carbon steel, with an inhibitor efficiency value of 92% at 293 K and a concentration of 100 ppm BPMDIB. The corrosion behavior of steel in 3.5% NaCl without and with the inhibitor at different concentrations was investigated between 293 and 323 K in temperature. Potentiodynamic polarization demonstrated the mixed-type action of the inhibitor. The adsorption of BPMDIB on the surface of carbon steel was explained by the Langmuir adsorption model. Furthermore, molecular dynamics simulations and quantum chemical computations based on density functional theory were conducted to study the effect of BPMDIB on the corrosion of carbon steel and to validate the accuracy of the experimental results and determine the efficacious sites of adsorption.

Keywords: Corrosion inhibition; Potentiodynamic polarization; Langmuir isotherms; DFT; 2-aryl imidazo [2,1-b] benzothiazole derivative.

حسابات DFT ودراسة تجريبية لتثبيط تآكل الفولاذ الكربوني في الأوساط المالحة بواسطة مشتق جديد من 2-أريل إيميدازو[2،1-ب] بنزوثيازول

رحاب ماجد كبة ، ندى محمد الجبوري*، نعيمة جبار اللامي
قسم الكيمياء، كلية العلوم، جامعة بغداد،بغداد، العراق

الخلاصة

تهدف هذه الدراسة إلى التحقق من كفاءة تثبيط مشتق جديد من 2-أريل إيميدازو[2،1-ب] بنزوثيازول و هو 2- (4-بروموفينيل-4-ييل)-5-يل-ميثيلين-3- (ب-توليل 2- -(فينيل- (3،5-ثنائي هيدروإيميدازولين-4-اون) إيميدازو [2،1-ب] بنز[د] ثيازول (BPMDIB).تم استخدام الحسابات الكيميائية لميكانيك الكم لدراسة تأثير المثبط على تآكل الفولاذ الكربوني. أظهرت النتائج أن زيادة تركيز المثبط أدى إلى

*Email: nada.mohammed@sc.uobaghdad.edu.iq

انخفاض كبير في معدل تآكل الفولاذ الكربوني، حيث بلغت قيمة كفاءة المثبط 92% عند 293 كلفن وتركيز 100 جزء في المليون من BPMDIB. تمت دراسة سلوك تآكل الفولاذ في كلوريد الصوديوم 3.5% بعدم وجود ومع وجود المثبط بتراكيز مختلفة عند نطاق درجة حرارة 293–303 كلفن. أظهر الاستقطاب الديناميكي الجهدي أن المثبط من النوع المختلط. وصف نموذج امتزاز BPMDIB على سطح الفولاذ الكربوني من نوع امتزاز Langmuir. تم أيضا إجراء عمليات محاكاة للديناميكيات الجزيئية وحسابات ميكانيك الكم الكيميائية بناءً على نظرية الكثافة الوظيفية لدراسة تأثير BPMDIBعلى تآكل الفولاذ الكربوني للتحقق من دقة النتائج التجريبية و لتحديد المواقع الفعالة للامتزاز.

1. Introduction

Corrosion refers to the deterioration or degradation of metals and alloys caused by their reaction with the surrounding environment through chemical or electrochemical processes [1]. Carbon steel has many applications in industries because of its abundance and high mechanical strength at a low cost [2-5]. There are many protective methods that have been utilized to safeguard the metal from corrosion, one of these methods was the addition of corrosion inhibitors, it is considered an excellent method for protecting against corrosion due to its ease and high efficiency [6-8]. The investigated inhibitor's job is to reduce the amount of metal corrosion by making the metal more resistant to corrosion, preventing substances from disseminating across its surface, altering the anodic or cathodic reactions, and enhancing the absorption of particles or ions on the metal's surface [9-10]. It is well known that all kinds of organic compounds of interest in electronics, optics, biology, material sciences, pharmacology, and so on, contain heterocycles in their building blocks. Researchers interested in Sulfur and nitrogen-containing heterocyclic compounds through decades by developing new procedures for organic synthesis [9-10]. Such moieties as thiazoles and imidazoles are reported as pharmacologically active compounds [11-12]. The corrosion reaction's mechanism and the chemical puzzle's solution were both clarified by theoretical computations [13-16].

Chemical uncertainty was resolved and the mechanism of reaction was elucidated through theoretical computations. Quantum chemical computational techniques can be employed to conduct theoretical calculations and ascertain the structural and electronic properties of the inhibitor molecules [17-18]. This study focuses on BPMDIB, a heterocyclic compound with significant pharmacological properties, which belongs to the class of 2-aryl imidazo[2,1-b] benzothiazole derivatives, as illustrated in Figure 1. Determining the inhibitor BPMDIB's efficiency of inhibition was the aim of this work, which Naeemah Al-Lami and colleagues prepared [19]. This was achieved both theoretically and experimentally, theoretically by using quantum chemical calculations based on density functional theory, Gaussian 09 program with (6-311/ B3LYP++G (2d, 2p)) level, this program was used to measure these theoretical calculations in (vacuum, DMSO, and H_2O) media, on the other hand, Practical measurements were conducted in a salty solution (3.5% NaCl) using the potentiostatic method [20-21].

2. Experimental part

2.1. Preparation of the carbon steel specimens

A bar of carbon steel metal marked C45 is formed from the following proportional constituents of metal materials: 0.122% C, 0.641% Mn, 0.206% Si, 0.016% P, 0.02% Mo, 0.031% S, 0.118% Cr, 0.451% Cu, and 0.105% Ni [2]. A carbon steel bar is segmented into several specimens to form a carbon steel disc sample with a 3 mm thickness and 1.6 cm diameter. silicon carbide (SiC) paper with different grades was used to refined metal samples, then washed with water, distilled water and degreased with acetone, rinsed again with

distilled water, and lastly stored in a desiccator after it was dehydrated at room temperature [11].

2.2 Preparation of solutions

2.2.1 Preparation of Blank solution

Thirty-five grams of salt (NaCl) salt were dissolved in 100 milliliters of distilled water to create a brine solution with a concentration of 3.5% NaCl. This solution was then transferred to a 1000-milliliter volumetric flask, where it was mixed with 6 milliliters of DMSO solvent. The solution was then brought to a final volume of 1 liter with the addition of distilled water.

2.2.2 Preparation of the BMTDIB concentrations

Dissolving (0.01, 0.05, and 0.1) g of BMTDIB inhibitor in 6 mL of DMSO to prepare 10, 50, and 100 ppm concentrations of it, respectively, then added these solutions to one-liter volumetric flask containing 35gm of NaCl salt (3.5%), dissolved with distilled water then complete the volume of each solution to (1 L) with distilled water.

3. Results and discussion

3.1. Electrochemical measurements

3.1.1 Potentiostatic polarization study

Potentiodynamic polarization measurements were used to characterize the corrosion effect on the metal surface in salty solutions in the presence and absence of BPMDIB organic inhibitor, varying in dosage. The potentiostatic system consist of host computer with M lab software, thermostat, potentiostat and magnetic stirrer. The most important component of this system was the corrosion cell, which is fabricated of Pyrex and has a capacity of one liter. The corrosion cell is primarily composed of three electrodes: the reference electrode, which is positioned close to the working electrode, it was employ to monitor the voltage of the working electrode, which is represented by a carbon steel sample with a surface area of 1 cm. Ag/AgCl, was the silver-silver chloride reference electrode, used to validate a steady state open circuit potential (Eocp) [7, 20], the working electrode was immersed in the blank solution for 15 minutes, this is the shortest period of time to achieve equilibrium for the ions in the reaction medium. In the range of (±200 mV), It was observed that this potential initiated the electrochemical measurements. All test solutions were run at the following temperatures: (293, 303, 313, and 323) K.

3.2. Quantum chemical calculations

Density functional theory (DFT)-based quantum chemical calculations offered a very helpful tool for comprehending the structural makeup, molecular characteristics, and atom-by-atom behavior of the organic inhibitor BPMDIB. Theoretical corrosion inhibition parameters were used to investigate the inhibition efficiencies of this compound. These parameters include the Lowest Unoccupied Molecular Orbital (E_{LUMO}), the Highest Occupied Molecular Orbital (E_{HOMO}), energy gap (E_{gap}) between E_{HOMO} and E_{LUMO}, electron affinity (A), dipole moment (μ), ionization energy (IP), global hardness (η), softness (S), global electrophilicity (ω), electronegativity (χ), fraction of electrons transferred (ΔN), and total energy (E_{tot}) [7].

3.3. Molecular geometry

Two-dimensional structure of BPMDIB inhibitor compound was build by using Chem-Draw software within the Mopac program, resulting in a clear atomic numbering scheme, as depicted in Figure 1a. he fully optimized structure of inhibitor in vacuum was carried out by

using Gaussian 09 program based on DFT with 6-311++G/(2d, 2p) level of theory [13]. Figure 1b shows the optimize structure in three dimension of the studied inhibitor BPMDIB.

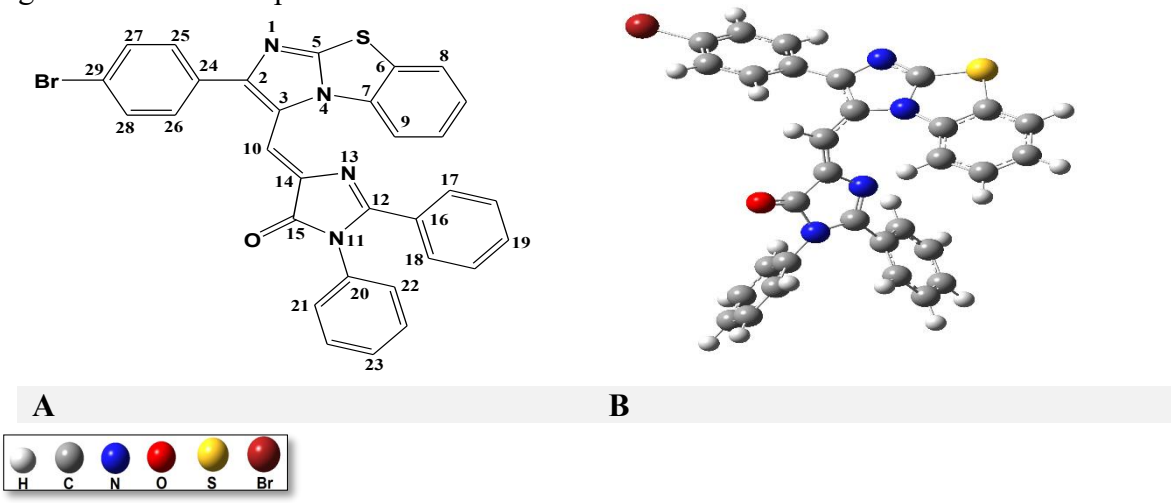

Figure 1: a. 2D structure of BPMDIB with the numbering atomic structure and b. 3D, the optimized structure of the BPMDIB inhibitor calculated by DFT method with a 6-311++G (2d, 2p) level of theory.

The geometric structure of the organic inhibitor BPMDIB was shown in Table 1. The optimal geometric structure is nearly ideal. Table 1 clearly demonstrates that in the BPMDIB complex, C29-Br has the longest bond length (1.8679 Å). C-S, C-N, and C-C bonds undergo slight expansion or contraction depending on the groups that are attached to them and donate or withdraw electrons. As shown, the compound is not planar, based on the dihedral angles (cis & trans) values, with C1 point group, (dihedral angles distant from 0.00 and dihedral angles deviating from 180.00 degrees) [7].

Table 1: The geometrical structure of BPMDIB inhibitor calculated by DFT in vacuum

Bond	Bond length (Å)	Angle	Angle (degree)	Dihedral angle	Dihedral angle (degree)
N1-C2	1.4005	**C2N1C5**	108.239	**C5N1C2C24**	179.2022
C2-C3	1.4599	**C3C2C24**	129.302	**C2N1C5N4**	1.1717
C3-C4	1.4045	**N4C3C2**	105.168	**C2N1C5S**	-176.8624
N4-C5	1.4200	**C3N4C5**	108.577	**N1C5N4C3**	-0.9288
N4-C7	1.4878	**C3N4C7**	138.931	**C5N4C7C9**	175.5967
C5-S	1.7490	**N4C5S**	114.078	**C5N4C7C6**	-3.5413
C6-S	1.7713	**N1C5N4**	108.415	**C5SC6C8**	-178.3172
C6-C7	1.4182	**SC6C7**	114.157	**C5SC6C7**	0.7589
C10-H	1.1058	**N4C7C6**	110.755	**N1C2C24C25**	29.4364
C10-C14	1.3413	**C3C10H**	114.552	**C25C27C29Br**	-179.9940
N11-C12	1.4455	**C3N10C14**	125.830	**C25C27C29C28**	-0.01091
N11-C15	1.4621	**C12N11C15**	107.028	**N4C3C10H**	130.4462
N11-C20	1.4498	**C12N11C20**	123.036	**C3C10C14C15**	-177.3644
C12-N13	1.3204	**N11C12N13**	111.186	**C3C10C14N13**	-0.3395
C12-C16	1.4647	**C12N13C14**	109.947	**C10C14C15N11**	-179.8912
N13-C14	1.3923	**N11C15O**	124.442	**C10C14C15O**	-2.2020
C15-O	1.2110	**N11C15C14**	104505	**N13C12C16C18**	137.3540
C29-Br	1.8679	**C27C29Br**	118.257	**C16C12N11C20**	-28.7507

The molecular orbital density distributions of BPMDIB's highest occupied molecular orbital (HOMO) and lowest unoccupied molecular orbital (LUMO) are visualized in Figure 2, providing insight into the compound's electronic structure. At the ideal geometry of the investigated BPMDIB inhibitor in vacuum, HOMO and the LUMO intensity distributions are mostly found on the moieties of [2-(4-bromophenyl) imidazole(2,1-b) benzothiazoles] and [2-phenyl-3-en-phenimidazolin-4-one]. This suggests that most planar regions of the molecule contain the desired active sites for electrospinning [7,8], as shown in Figure 2. Demonstrate that the planar regions of the BPMDIB molecule are home to both the HOMO and LUMO.

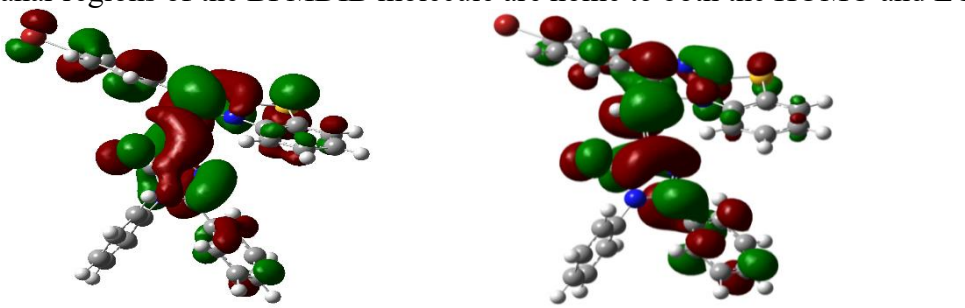

a- HOMO **b- LUMO**

Figure 2: The frontier molecular orbital density distributions of BPMDIB inhibitor HOMO and LUMO. [Red color: negatively charged lobe; green color: positive charge lobe].

3.4. Global molecular reactivity

The data presented in Tables 2a and 2b reveal that BPMDIB exhibits promising inhibitory properties, as evidenced by its favorable quantum corrosion efficiency parameters. Molecules with a higher EHOMO value are more likely to donate electrons to molecules with a lower empty molecular orbital energy, which are known as acceptor molecules. Another parameter was E_{LUMO}, lower value of E_{LUMO} indicate higher capability of accepting electrons. A higher value of E_{HOMO} leads to an increase in the inhibition efficiency of inhibitor and vice versa for E_{LUMO}, on the other hand, molecule with higher dipole moment value (μ) have higher adsorption capacity between the inhibitor molecule and metal surface [13]. Molecules with low values of (ionization potential) IP make an increase in the effectiveness of the inhibitor [20]. A high EA value indicates a less stable molecule, making it an effective corrosion inhibitor. An inhibitor with a low η value is considered a good organic inhibitor, as an increase in η reduces the stability of the inhibitor. Molecules that have a higher value of chemical softness (S)having good inhibition capacity. Molecules with low electronegativity value (χ) classified as a good inhibitor. Higher value of global electrophilicity index (ω) reflecting a good inhibition ability of inhibiter. ΔN value shows the ability of BPMDIB inhibitor to get electrons from metal surface in the unoccupied orbital (3d) [22], this ability enhances the inhibition efficiency (IE) [23-25]:

$$\Delta E_{gap} = E_{LUMO} - E_{HOMO} \quad (1)$$

$$IP = -E_{HOMO} \quad (2)$$

$$EA = -E_{LUMO} \quad (3)$$

$$\chi = (IP + EA)/2 \quad (4)$$

$$\eta = (IP - EA)/2 \quad (5)$$

$$S = 1/\eta \quad (6)$$

$$\omega = (-\chi)^2/2\eta = \mu^2/2\eta \quad (7)$$

$$\Delta N = (\chi_{Fe} - \chi_{inhib.})/[2(\eta_{Fe} + \eta_{inhib.})] \quad (8)$$

Where χ_{Fe}= 7, while η_{Fe}=0 for bulk iron atom [6]. If ΔN> 0, the corrosion inhibitor transfers its electrons to metal and vice versa if ΔN< 0.

Table 2a- DFT calculations results for some physical properties of BPMDIB compound studied at the optimized structure

Inhib. Medium	*Point Group*	*Molecular formula*	E_{HOMO} *(eV)*	E_{LUMO} *(eV)*	ΔE_{gap} *(eV)*	*μ (Debye)*	E_{total} *(eV)*
Vacuum	C_1	$C_{31}H_{19}N_4OSBr$	-5.7335	-2.7674	2.9661	7.2902	-121355.727

Table 2b- Theoretical parameters for BPMDIB compound studied at the optimized structure

Inhib. Medium	*IP (eV)*	*EA (eV)*	□ *(eV)*	□ *(eV)*	*S (eV)*	*ω (eV)*	□□
Vacuum	5.7335	2.7674	1.4830	4.2504	0.6743	6.0909	0.9270

3.5. Active sites of the BMTDIB inhibitor

Frontier molecular orbital density distributions HOMO and LUMO diagrams (Figure 2) of the BMTDIB inhibitor explained that the electron densities were not spread homogeneously throughout the molecule. DFT Mulliken charges population analysis was employed at the (6-311++G (2d, 2p)) level of theory to elucidate the importance of the reactive centers of the BPMDIB compound, specifically the nucleophilic and electrophilic reactive site centers, as reported in [26]. Figure 3, in which the color ranges from light red (atoms carrying the largest negative values of charge) to light green (atoms carrying the largest positive values of charge). The black color in the middle represents atoms of zero charge. The more negative charge atom of the adsorbed inhibitor was the more easily it donated its electrons to the unoccupied orbital and adsorbed preferably on the metal surface. It is evident from Table 3 that nitrogen, sulfur, oxygen, and some carbon atoms that carry the highest negative charges could donate their electrons to the carbon steel surface to form coordinate bonds, contingent upon the orientation of the optimized structure of the inhibitor in three-dimensional space. These donation and back-donation processes strengthen the adsorption of BPMDIB onto the carbon steel surface and increase the inhibition efficiency.

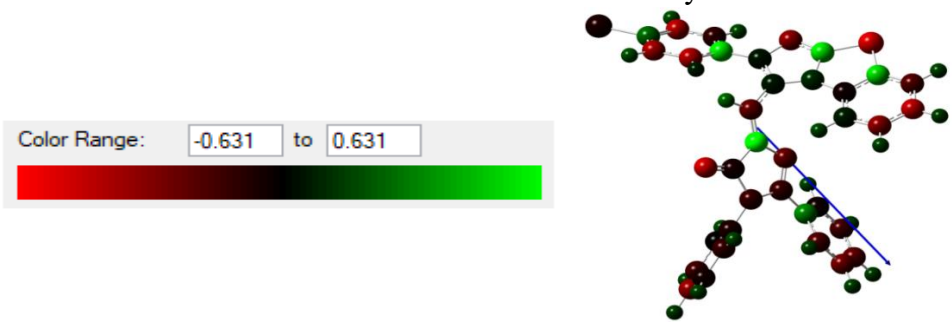

Figure 3: Distribution of Mulliken charges according to the color of the charge on the atoms along with the direction of the net dipole moment.

Table 3: The mulliken charge population analysis of BPMDIB compound studied by DFT in vacuum

Atom No.	*Electronic Charge (ecu)*	*Atom No.*	*Electronic charge (ecu)*	*Atom No.*	*Electronic Charge (ecu)*	*Atom No.*	*Electronic Charge (ecu)*
N1	-0.290	***C8***	-0.172	***C16***	0.280	***C25***	-0.095
C3	0.053	***C10***	-0.207	***C18***	-0.162	***C26***	-0.362
N4	0.093	***N11***	-0.119	***C19***	-0.198	***C27***	-0.374
C5	0.483	***N13***	-0.203	***C21***	-0.107	***C28***	-0.344
S	-0.441	***C14***	0.631	***C23***	-0.301	***C29***	0.214
C6	0.455	***O***	-0.413	***C24***	0.504	***Br***	-0.058

ecu: electron control unit.

3.6. Corrosion inhibition measurement
3.6.1. Potentiodynamic Polarization Measurements

Table 4 shows the electrochemical corrosion parameters that calculated by Eqs (9–12). Figure 3 (a, b) displays the polarization curves of C.S in salty media with varying BMTDIB concentrations as well as the compound's ideal concentration) [7, 26-27]:

$$\%IE = \frac{i_{corr(un)} - i_{corr(in)}}{i_{corr(un)}} \times 100 \qquad (9)$$

where $i_{corr(in)}$ is the inhibited corrosion current density and $i_{corr(un)}$ is the uninhibited current density. Equation 10 can be used to calculate (R_p), the value of polarization resistance:

$$Rp = \frac{b_a \times b_c}{2.303(b_a + b_c) \times i_{corr}} \qquad (10)$$

Θ was calculated by "Eq. (11)", [26, 28]:

$$\theta = \frac{\%IE}{100} \qquad (11)$$

CR can be measured by "Eq. (12)", [29]:

$$CR = i_{corr} \times 0.249 \qquad (12)$$

Corrosion rate was decrease when BPMDIB inhibitor was added, that cause a shifts of the cathodic and anodic curves to a lower values of current densities, and both cathodic and anodic reactions of CS electrodes are inhibited by BPMDIB inhibitor in salty solution.
As shown in Table 4, a direct correlation was observed between temperature and corrosion rate ($I_{corr.}$), whereas the inhibition efficiency (IE%) increased with increasing inhibitor concentration. The optimal inhibition conditions for the BPMDIB inhibitor in saline media were found to be 293K and 100ppm, where the highest level of corrosion protection was achieved. These results are agreed to the lowest I_{corr} (17.10 μA cm^{-2}) and the highest IE% of 92%, Corrosion rate values have decreased with increasing concentration of BPMDIB inhibitor, that led to an increase in the cathodic and anodic $I_{corr.}$ without shifting the $E_{corr.}$ So, the inhibitor can be described as mixed-type inhibitor.

Table 4: Electrochemical results of CS corrosion in seawater at various concentrations of BPMDIB inhibitor.

Inhib. Conc.	*T (K)*	*E_{corr} (V)*	*i_{corr} ($\mu A.cm^{-2}$)*	*Bc ($V.dec^{-1}$)*	*ba ($V.dec^{-1}$)*	*CR (mm/year)*	*Θ*	*IE%*
***Blank* 0 ppm**	293	-0.529	228.9	0.189	0.100	1.222	-	-
	303	-0.534	237.8	0.073	0.192	1.265	-	-
	313	-0.452	255.1	0.102	0.158	1.350	-	-
	323	-0.574	269.6	0.168	0.113	1.421	-	-
10 ppm	293	-0.419	26.91	0.305	0.182	0.264	0.88	88
	303	-0.400	27.85	0.309	0.198	0.273	0.88	88
	313	-0.435	29.17	0.319	0.182	0.286	0.89	89
	323	-0.474	35.64	0.221	0.293	0.350	0.86	86
50 ppm	293	-0.613	19.34	0.266	0.175	0.190	0.91	91
	303	-0.623	21.18	0.283	0.197	0.208	0.91	91
	313	-0.619	31.86	0.365	0.263	0.313	0.87	87
	323	-0.524	33.94	0.378	0.250	0.333	0.87	87
100 ppm	293	-0.665	17.10	0.206	0.128	0.168	0.92	92
	303	-0.669	19.56	0.251	0.136	0.192	0.91	91
	313	-0.599	21.50	0.196	0.186	0.211	0.91	91
	323	-0.679	23.86	0.219	0.185	0.234	0.91	91

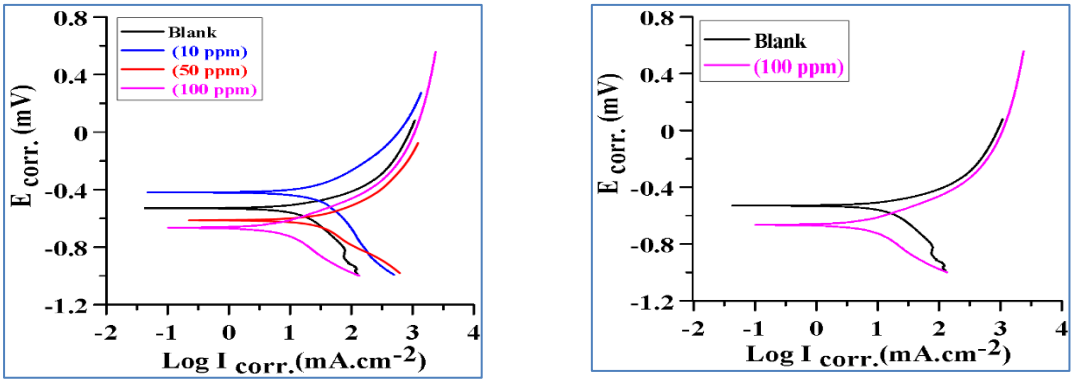

A **B**

Figure 4: carbon steel Polarisation curves seawater for BPMDIB compound (a) at various concentrations, and T (293 K), (b) at the optimum concentration of BPMDIB inhibitor, and T (293 K).

Figure 5 demonstrates a plot between the concentrations of the BPMDIB inhibitor and its inhibition efficiency for corrosion inhibition of carbon steel at a temperature of 293 K. The diagram indicates that the efficiency of inhibitor molecules in adsorption on the metal surface increases with increasing inhibitor concentration

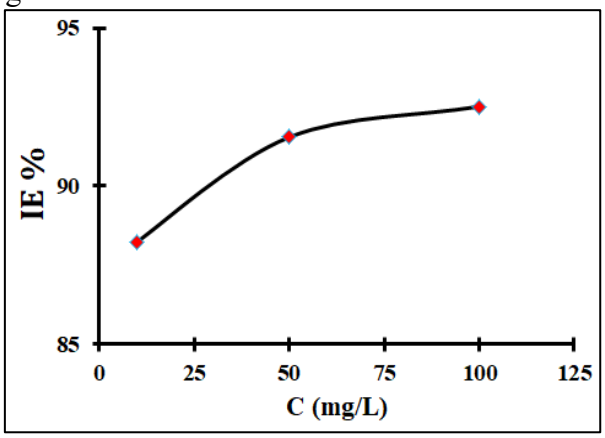

Figure 5: Inhibition efficiency IE% for C.S at different concentrations of BPMDIB inhibitor.

3.6.2. Thermodynamic activation parameters and Corrosion kinetic

According to the Arrhenius law, the corrosion rate logarithm follows a linear relationship, as illustrated by a straight line [30-31]. At various concentrations, activation coefficients were computed both with and without inhibitor, "Eq. (13)" was used to compute the pre-exponential factor (A) and the activation energy of the corrosion process (E_a). All of the E_a values are greater than the blank's (4.405 kJ/ mol) in the presence of a BPMDIB inhibitor, suggesting that the inhibitor is slowing down the corrosion reaction of C.S. These results support the physical reaction.

$$\text{Log } (I_{corr}) = \text{Log } A - E_a / 2.303RT \quad (13)$$

$$\text{Log } (I_{corr}/T) = \log (CR/T) = \text{Log } (R/N\,h) + \Delta S^*/2.303R - \Delta H^*/2.303RT \quad (14)$$

The activation thermodynamic parameters (ΔH^* and ΔS^*) for BPMDIB inhibitor were clearly shown in table 5, the nature for this reaction was an endothermic because of positive values of ΔH^*. Negative values of (ΔS^*) for the corrosion reaction indicate a decrease in the degree of freedom and a consequent inhibition action, "Eq. (15)" was used to calculate ΔG^* values, the adsorption process is not spontaneous because of positive values of ΔG^*.

$$\Delta G^* = \Delta H^* - T\Delta S^* \quad (15)$$

Table 5: Kinetic parameters of corrosion of CS in blank solution and with different concentrations of BPMDIB compound.

Conc. (ppm)	*ΔG* (kJ/ mol)*				*ΔH* kJ/ mol*	*ΔS* kJ/ mol K*	*Ea* kJ/ mol*	*A Molecule/ cm² S*
	293K	*303K*	*313K*	*323K*				
Blank 0	71.253	73.537	75.822	78.106	4.316	-0.228	4.405	8.3329E+26
10	77.284	79.741	82.198	84.655	5.296	-0.246	6.909	2.6650E+26
50	75.850	77.964	80.078	82.192	13.908	-0.211	16.492	9.8038E+27
100	85.628	88.018	90.409	92.799	15.593	-0.239	18.193	3.5620E+26

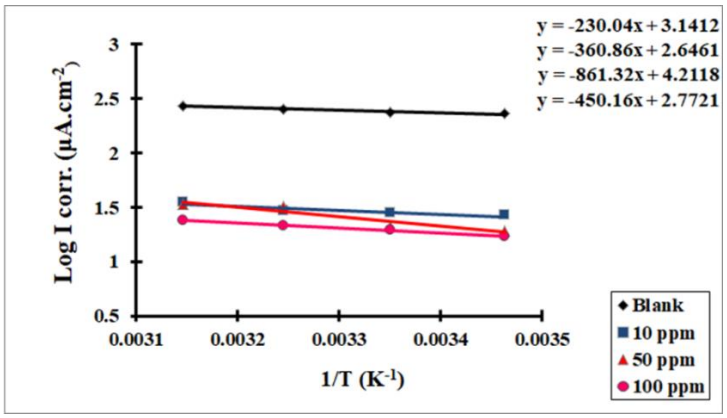

Figure 6: Plotting of the carbon steel log (I_{corr}) versus (1/ T) in saline media with and without BPMDIB inhibitor at various concentrations.

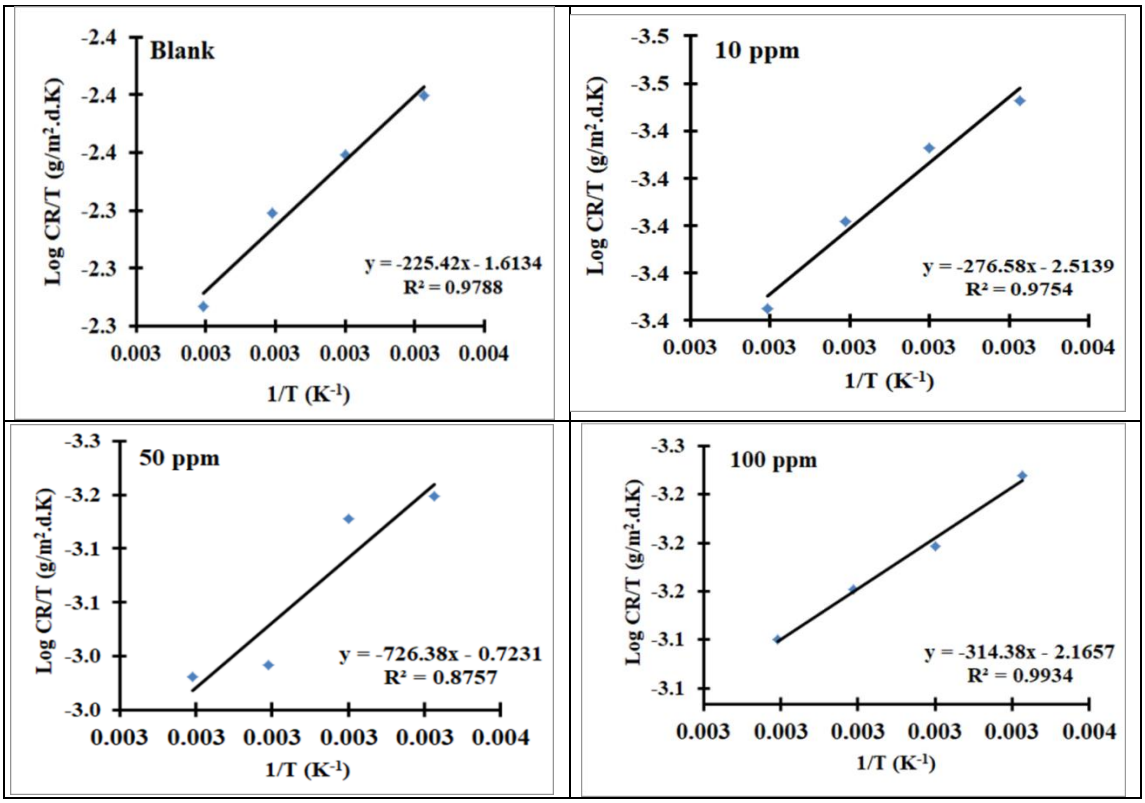

Figure 7: Plotting of log (CR/ T) versus (1/ T) of CS in saline media in blank solution and in the presence of various concentrations of the BPMDIB compound.

3.6.3. Adsorption isotherm

Adsorption isotherms are crucial in elucidating the reaction between the inhibitor molecule and the metal surface [32]. The isotherm that was widely used is Langmuir adsorption isotherm. It can be mathematically represented by the following equation:

$$C/ \Theta = (1/ K_{ads}) + C \quad (16)$$

Figure 8 shows a plot of C/θ against concentration C in salty solution for BPMDIB inhibitor; it can be used to determine K_{ads} (see Figure 9). Whereas C is the inhibitor concentration in the salty media, K_{ads} is the adsorption equilibrium constant. Equation 17 relates the adsorption equilibrium constant to the free energy of adsorption (ΔG_{ads}):

$$K_{ads}= (1/55.55) \exp (\Delta G_{ads}/ RT) \quad (17)$$

Where T is the absolute temperature (K), R is the gas constant (J K^{-1} mol^{-1}), and 55.5 is the molar concentration of water in the solution (mol L^{-1}). Equation 19 was used to express the Vant Hoff Equation slope, which yielded the enthalpy value of adsorption ($\Delta H°_{ads}$), and the intercept of the same equation yielded the entropy value of adsorption ($\Delta S°_{ads}$).

$$\Delta G°_{ads}= -2.303 RT \log K_{ads} \quad (18)$$

$$\Delta G°_{ads}= \Delta H°_{ads} - T\Delta S°_{ads} \quad (19)$$

$$\log K_{ads}= - \Delta H°_{ads}/ 2.303 RT + \Delta S°_{ads}/ 2.303 R \quad (20)$$

The organic inhibitor BPMDIB's thermodynamic functionalization on the C.S surface in saline media at diferent temperatures is listed in Table 6. The BPMDIB Langmuir isotherm's increased K_{ads} values indicate strong inhibitory adsorption effect on CS in saline media. A spontaneous adsorption process is indicated by negative values of $\Delta G°_{ads}$. Negative values of $\Delta G°_{ads}$ about -20 (kJ/mol) or less were ascribed to electron transfer, which causes a chemical bond to form (chemisorption); values of more positive than -20 (kJ/mol) were attributed to physical adsorption on the iron surface [6].

At different temperatures (293-323 K), the calculated values of $\Delta G°_{ads}$ in the salty medium were found to vary between -9.6448 and 9.1813) (kJ mol^{-1}). The corrosion process is entropically favorable because of positive values of $\Delta S°_{ads}$. These findings show that a physical adsorption process is used to conduct the BPMDIB adsorption [7]. The exothermic nature of the inhibitory molecule adsorption process on the C.S surface is indicated by the negative value of $\Delta H°_{ads}$ in the salt media. Table 6 shows that the ΔH^{o}_{ads} of the BPMDIB compound in the salt medium are -4.9977 (kJ mol^{-1}).

Table 6: Thermodynamic parameters of BPMDIB adsorption on metal surface in salty media at various temperatures.

T (K)	*K_{ads} ($L\ mol^{-1}$)*	*$\Delta G°_{ads}$ ($kJ.\ mol^{-1}$)*	*$\Delta H°_{ads}$ ($kJ.mol^{-1}$)*	*$\Delta S°_{ads}$ ($kJ.mol^{-1}$)*	*R^2*
293	$53.8251*10^4$	-9.6448	-4.9977	0.1260	1.0000
303	$50.6014*10^4$	-9.4917			1.0000
313	$47.0062*10^4$	-9.3091			0.9992
323	$44.6428*10^4$	-9.1813			0.9994

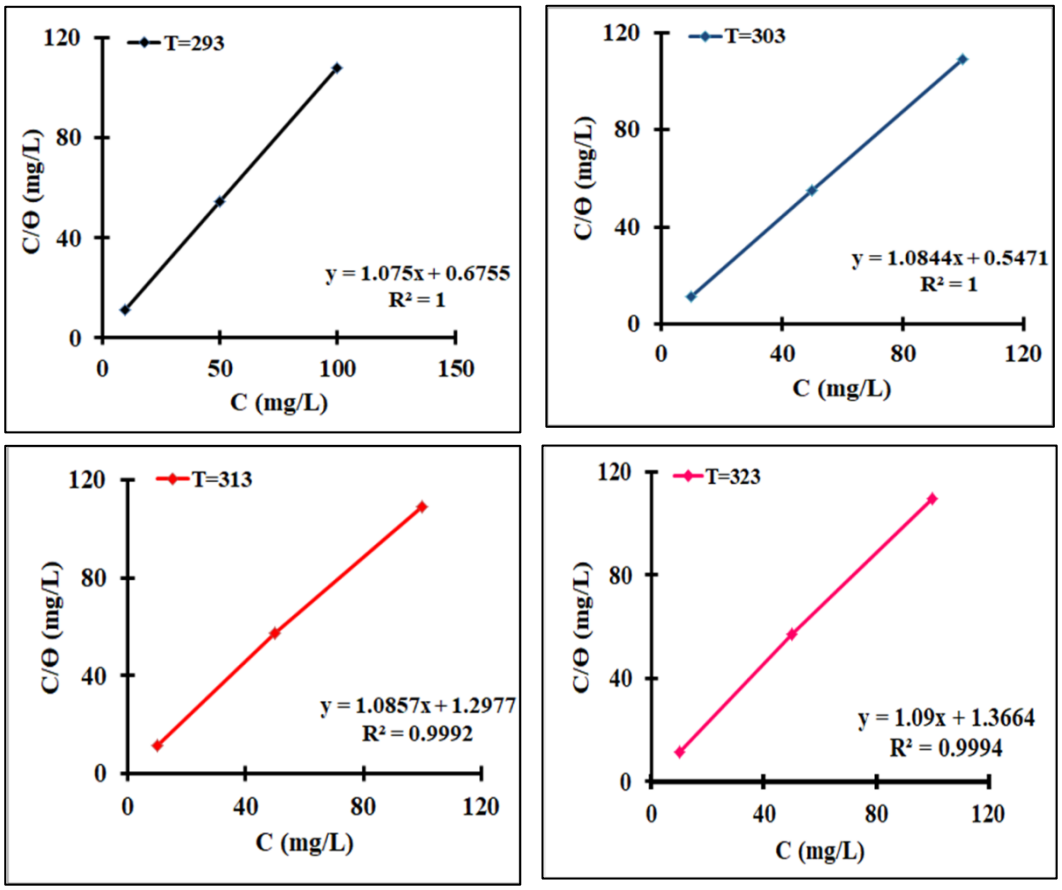

Figure 8: Langmuir isotherms plot for the adsorption BPMDIB inhibitor on CS in the saline media at different temperatures

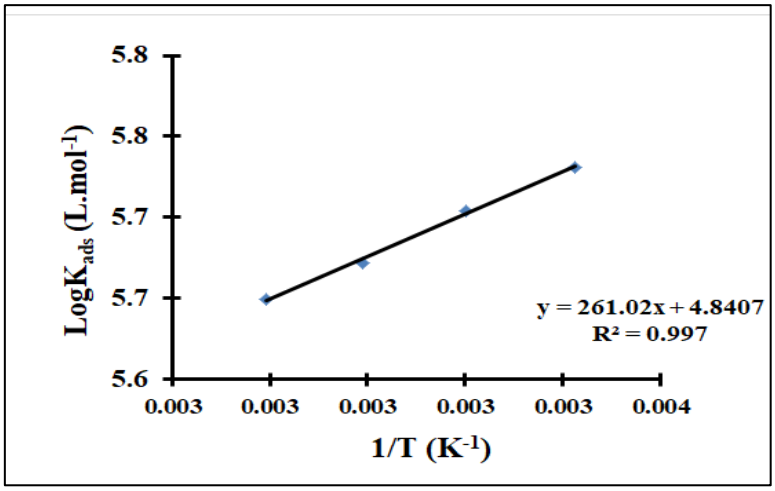

Figure 9: Plotting of (log K_{ads}) against (1/ T) for BPMDIB inhibitor.

Conclusion

A new derivative (BPMDIB) was studied theoretically and experimentally as corrosion inhibitor. Furthermore, Theoretical calculations based on density functional theory and electronic parameters shows proved that the BPMDIB is a good organic inhibitor of corrosion of carbon steel surfaces, and this was further supported by the results. In addition, experimental studies using potentiodynamic polarization measurements showed very good efficiency of the studied inhibitor against surface corrosion of carbon steel. Accordingly, the corrosion inhibition efficiency of this compound was (92%) at a temperature of 293 K and the optimal concentration of BPMDIB is 100 ppm. Moreover, the values of the charge transfer resistance increased in the presence of (BPMDIB) in EIS tests, indicating that they can protect steel from corrosion by forming a robust protective film. Additionally, the inhibition efficiency for the BPMDIB compound was found to be decreased with increased temperature and increased with increasing the inhibitor concentration (physisorption inhibition). The high values of K_{ads} obtained from the Langmuir isotherm give an indication of strong adsorption of BPMDIB inhibitor on the carbon steel surface in saline water, and this was supported by the negative values of $\Delta G°ads$, which indicate a spontaneous adsorption process.

Reference

[1] A. Kadhim, A. A. Al-Amiery, R. Alazawi, M. K.S. Al-Ghezi, and R. Abass. "Corrosion inhibitors. A review", *International Journal of Corrosion and Scale Inhibition,* Vol. 10, No 1, pp. 54-67, 2021.

[2] H. Parangusan, MH. Sliem, AM. Abdullah, M. Elhaddad, N. Al-Thani and J. Bhadra. "Plant extract as green corrosion inhibitors for carbon steel substrate in different environments: A systematic review", *International Journal of Electrochemical Science*, Vol. 20, No. 4,PP.1-11,2025.

[3] H. Assad, S. Kumar, S. K. Saha, N. Kang, I. Fatma, H. Dahiya*, et al.* "Evaluating the adsorption and corrosion inhibition capabilities of Pyridinium-P-Toluene Sulphonate on MS in 1 M HCl medium: An experimental and theoretical study", *Inorganic Chemistry Communications,* Vol. 153, pp. 110817, 2023.

[4] F. El-Hajjaji, E. Ech-Chihbi, N. Rezki, F. Benhiba, M. Taleb, and D. S. Chauhan, "Electrochemical and theoretical insights on the adsorption and corrosion inhibition of novel pyridinium-derived ionic liquids for mild steel in 1 M HCl", *Journal of Molecular Liquids,* Vol. 314, pp. 113737, 2020.

[5] G. K. P. Barboza, M. C. C. de Oliveira, M. A. Neves and A. Echevarria. "Justicia brandegeeana as a green corrosion inhibitor for carbon steel in sulfuric acid". *Green Chemistry Letters and Reviews*, Vol. 17, No. 1,pp.1-18, 2024.

[6] S. Xu, S. Zhang, L. Guo, L. Feng, and B. Tan. "Experimental and theoretical studies on the corrosion inhibition of carbon steel by two indazole derivatives in HCl medium", *Materials,* Vol. 12, pp. 1339, 2019.

[7] R. M. Kubba, M. A. Mohammed, and L. S. Ahamed. "DFT calculations and experimental study to inhibit carbon steel corrosion in saline solution by Quinoline-2-One derivative", *Baghdad Science Journal,* Vol. 18, No. 1, pp. 113-123, 2020.

[8] X. Li, S. Deng, T. Lin, X. Xie, and X. Xu. "Inhibition action of triazolyl blue tetrazolium bromide on cold rolled steel corrosion in three chlorinated acetic acids", *Journal of Molecular Liquids,* Vol. 274, pp. 77-89, 2019.

[9] S. Kumar, V. Kalia, M. Goyal, G. Jhaa, S. Kumar, and H. Vashisht*,* "Newly synthesized oxadiazole derivatives as corrosion inhibitors for mild steel in acidic medium: Experimental and theoretical approaches", *Journal of Molecular Liquids,* Vol. 357, pp. 119077, 2022.

[10] C. Verma and M. Quraishi. "Recent progresses in Schiff bases as aqueous phase corrosion inhibitors: Design and applications", *Coordination Chemistry Reviews,* Vol. 446, p. 214105, 2021.

[11] N. Etivand, M. Ahmadi Sabegh, and J. Khalafy. "Synthesis of a new series of benzo [d] imidazo [2, 1-b] thiazole-1-ium hydroxides by a one-pot, three-component reaction in water", *Monatshefte für Chemie-Chemical Monthly,* Vol. 150, pp. 317-325, 2019.

[12] M. Al-Jamal and N. Al-Lami. "Antimicrobial activities of some new heterocyclic compounds bearing imidazo [2, 1-b] benzothiazole moiety" in *AIP Conference Proceedings*, 2023.

[13] R. M. Kubba, M. A. Mohammed, and L. S. Ahamed. "DFT calculations and experimental study to inhibit carbon steel corrosion in saline solution by Quinoline-2-One derivative", *Baghdad Science Journal,* Vol. 18, No 1, 2021.

[14] Y. Youssefi, L. Oucheikh, O. Ou-ani, M. Jabha, A. Oubair, M. Znini, E.E. Ebenso, B. Hammouti. "Synthesis, characterization and corrosion inhibition potential of olefin derivatives for carbon steel in 1M HCl: Electrochemical and DFT investigations", *Moroccan Journal of Chem*istry, Vol 11, No (1), pp. 155-187, 2023.

[15] M. Farrokhnia. "Density Functional Theory studies on the antioxidant mechanism and electronic properties of some bioactive marine meroterpenoids: Sargahydroquionic acid and sargachromanol", *American Chemical Society omega*, Vol 5, No 32, PP. 20382–20390, 2020.

[16] B. Anandkumar, N.G.Krishna, R.V.Solomon, T.Nandakumar and J.Philip. "Synergistic enhancement of corrosion protection of carbon steels using corrosion inhibitors and biocides: Molecular adsorption studies, DFT calculations and long-term corrosion performance evaluation". *Journal of Environmental Chemical Engineering*, *11*(3), 109842, 2023.

[17] J. D. Hidary. "Quantum Computing: An Applied Approach". 2nd. ed: *Springer,* 2021.

[18] M. En-Nylly, S. Skal,Y. Elaoufir, H. Lgaz, R. J. Adnin and A. A. Alrashdi. "Performance evaluation and assessment of the corrosion inhibition mechanism of carbon steel in HCl medium by a new hydrazone compound: Insights from experimental, DFT and first-principles DFT simulations", *Arabian Journal of Chemistry*, 16(6), 104711. 2023.

[19] E. Aquino-Torres, R. L . Camacho- Mendoza, E. Gutierrez, J. A. Rodriguez, L. Feria and p. Thangarasu. "The influence of iodide in corrosion inhibition by organic compounds on carbon steel: Theoretical and experimental studies", *Applied Surface Science*, 514, 145928, 2020.

[20] Yu. Ozawa. "Computational investigation on copper (I)-catalyzed enantioselective radical borylation of benzyl halides", in copper (I)-catalyzed stereoselective borylation reactions: multisubstituted alkenyl and allylic boronates, ed: *Springer*, pp. 213-223, 2023.

[21] M. H. Al-Jamal, N. Al-Lami, and R. M. Al-Azy. "Synthesis of new S, N, O-alkylated benzo [d] imidazo [2, 1-b] thiazole and the study of their biological applications", in *AIP Conference Proceedings*, pp. 020108, 2020.

[22] A. Ganash, S. Alsayed, and A. H. Al-Moubaraki. "Anticorrosive properties of aqueous Cichorium intybus seeds extract as a sustainable-green inhibitor for aluminum corrosion in hydrochloric acid solution: An experimental and DFT/MC/MD theoretical approach", *Journal of Environmental Chemical Engineering,* Vol. 11, pp. 110227, 2023.

[23] J. Duboscq, R. Sabot, M. Jeannin, and P. Refait. "Localized corrosion of carbon steel in seawater: Processes occurring in cathodic zones", *Materials and corrosion,* Vol. 70, No 6, pp. 973-984, 2019.

[24] I. F. F. Orbitals. "Organic Chemical Reactions John Wiley and Sons", *New York,* 1976.

[25] R. Hsissou, A. El Mahmoudi, I. Saber, Z. Safi, M. El Faydy, F. Benhiba, *et al.* "Theoretical and experimental investigation for mild steel in acidic environment using isoxazole sulfonamide derivatives as anticorrosion inhibitors", *Next Materials*, Vol. 9:101011,pp.1-19,2025.

[26] RM. Kubba and NM .Al-Joborry. "Theoretical and experimental study of a new imidazo (1, 2-a) pyridine derivative as a corrosion inhibitor for the carbon steel surface in the saline media". *Al-Nahrain Journal of Science*, Vol. 23, No. 1, pp. 13-26, 2020.

[27] S. Sadiq, Al-tamimi Amaal, and O. Entesar. "Synthesis, Characterization and Investigation of New Polymer Contain Heterocyclic Derivatives as Corrosion Inhibitor for Stainless steel in acidic medium", *European Journal of Molecular & Clinical Medicine*, 7(2), 2020.

[28] X. Liu, M. Gong, Sh. Deng, T. Zhao, T. Shen and J. Zhang. "Transforming damage into benefit: corrosion engineering enabled electrocatalysts for water splitting", *Advanced Functional Materials*, 31(11), 2009032, 2021.

[29] S. Harsimran, K. Santosh and K. Rakesh. "Overview of corrosion and its control: A critical review", *Proceedings on Engineering Sciences*, 3(1), 13-24, 2021.

[30] S. Habeeb and H. Almashhadani. "Synthesis of polysulfanilamide by electro polymerization and its corrosion protective properties on 316L stainless steel in 0.2 M HCl", *International Journal of Corrosion and Scale Inhibitio,* Vol. 11, No 2, pp. 621-632, 2022.
[31] S. Al-Mhyawi. "Application of expired Tramadol medicinal drug for corrosion inhibition of steel in acidic environment: analytical, kinetic, and thermodynamic studies", *International Journal of Corrosion and Scale Inhibitio,* Vol. 11, No 3, pp. 862-888, 2022.
[32] A. Kokalj. "On the use of the Langmuir and other adsorption isotherms in corrosion inhibition", *Corrosion Science,* Vol. 217, No 14, pp. 111112, 2023.